Neurochemical Research (2022) 47:1255–1268
https://doi.org/10.1007/s11064-021-03519-3

ORIGINAL PAPER

Effects of Chronic Arginase Inhibition with Norvaline on Tau Pathology and Brain Glucose Metabolism in Alzheimer's Disease Mice

Baruh Polis[1] · Margherita Squillario[2] · Vyacheslav Gurevich[1,4] · Kolluru D. Srikanth[1,3] · Michael Assa[1,4] · Abraham O. Samson[1]

Received: 29 August 2021 / Revised: 11 December 2021 / Accepted: 27 December 2021 / Published online: 31 January 2022

Abstract

Alzheimer's disease (AD) is an insidious neurodegenerative disorder representing a serious continuously escalating medico-social problem. The AD-associated progressive dementia is followed by gradual formation of amyloid plaques and neurofibrillary tangles in the brain. Though, converging evidence indicates apparent metabolic dysfunctions as key AD characteristic. In particular, late-onset AD possesses a clear metabolic signature. Considerable brain insulin signaling impairment and a decline in glucose metabolism are common AD attributes. Thus, positron emission tomography (PET) with glucose tracers is a reliable non-invasive tool for early AD diagnosis and treatment efficacy monitoring. Various approaches and agents have been trialed to modulate insulin signaling. Accumulating data point to arginase inhibition as a promising direction to treat AD via diverse molecular mechanisms involving, *inter alia*, the insulin pathway. Here, we use a transgenic AD mouse model, demonstrating age-dependent brain insulin signaling abnormalities, reduced brain insulin receptor levels, and substantial energy metabolism alterations, to evaluate the effects of arginase inhibition with Norvaline on glucose metabolism. We utilize fluorodeoxyglucose whole-body micro-PET to reveal a significant treatment-associated increase in glucose uptake by the brain tissue in-vivo. Additionally, we apply advanced molecular biology and bioinformatics methods to explore the mechanisms underlying the effects of Norvaline on glucose metabolism. We demonstrate that treatment-associated improvement in glucose utilization is followed by significantly elevated levels of insulin receptor and glucose transporter-3 expression in the mice hippocampi. Additionally, Norvaline diminishes the rate of Tau protein phosphorylation. Our results suggest that Norvaline interferes with AD pathogenesis. These findings open new avenues for clinical evaluation and innovative drug development.

Keywords Functional brain imaging · Glucose uptake · Energy metabolism · Tau protein · Insulin receptor · GLUT3

Abbreviations

AD	Alzheimer's disease
3×Tg	Triple-transgenic mouse model of Alzheimer's disease
PET	Positron emission tomography
CT	Computed tomography
Aβ	Amyloid-beta
NFT	Neurofibrillary tangles
CNS	Central nervous system
GLUT	Glucose transporter
WT	Wild-type
KEGG	Kyoto Encyclopedia of Genes and Genomes
BCAA	Branched chain amino acid
OD	Optical density
ANOVA	Analysis of variance
HDAC	Histone deacetylase
mTOR	Mechanistic Target of Rapamycin
S6K1	Ribosomal S6 kinase 1
PDPK1	3-Phosphoinositide-dependent protein kinase-1
AKT	RAC-alpha serine/threonine-protein kinase
CA	Cornus Ammonis

✉ Baruh Polis
baruhpolis@gmail.com

[1] Drug Discovery Laboratory, The Azrieli Faculty of Medicine, Bar-Ilan University, 1311502 Safed, Israel

[2] Department of Computer Science, Bioengineering, Robotics and System Engineering (DIBRIS), University of Genoa, Genoa, Italy

[3] Laboratory of Molecular and Behavioral Neuroscience, The Azrieli Faculty of Medicine, Bar-Ilan University, Safed, Israel

[4] The Azrieli Faculty of Medicine, Bar-Ilan University, Safed, Israel

SEM Standard error of the mean
mRNA Messenger ribonucleic acid

Introduction

Alzheimer's disease (AD) is a severe chronic neurodegenerative disorder and the most prevalent cause of dementia [1]. AD-associated cognitive decline is followed by brain atrophy, characteristic β-amyloid plaque deposition, and the formation of intracellular neurofibrillary tangles (NFTs) [2]. Of note, hyperphosphorylated microtubule-associated τ-protein (Tau) is a major component of neurofibrillary lesions stamping AD and several other brain pathologies that manifest in clinical dementia.

Accruing evidence indicates that AD is a complex metabolic disease with molecular and biochemical characteristics corresponding to diabetes mellitus and other metabolic disorders [3, 4]. Notably, brain glucose utilization is substantially reduced in the early stages of AD [5], contributing to disease pathogenesis. Human functional imaging studies utilizing fluorodeoxyglucose positron emission tomography (FDG-PET) consistently demonstrate glucose uptake decline in the brains of AD patients [6, 7], indicating PET as a reliable diagnostic method.

Additionally, human postmortem and animal studies demonstrated AD-associated brain insulin resistance and reduced insulin receptor (IR) expression [8], which has led to the hypothesis that AD is a distinctive form of diabetes (type 3) with selective involvement of the brain, and molecular and biochemical features overlapping with both diabetes type 1 and type 2 [9].

Insulin of pancreatic origin is vital for general glucose, fat, and protein metabolism. Its primary physiological function is to enhance glucose uptake by the cells [10]. For a long time, the brain has not been considered as an insulin target tissue; however, current evidence firmly indicates insulin involvement in brain function [11]. Remarkably, being extremely energetically active, the brain has been viewed as an organ metabolizing glucose independently of insulin. However, in addition to IR, the expression of the insulin-sensitive glucose transporter-4 (GLUT4), typical in peripheral tissues, has been credibly demonstrated in the central nervous system (CNS) [12]. Nevertheless, insulin-independent glucose transporter 3 (GLUT3) and glucose transporter 1 (GLUT1) are more ubiquitous in the brain and highly expressed in axons and dendrites [13]. These predominant isoforms present with a ratio of seven to one [14], and GLUT3 are the fastest high-affinity glucose transporters in the CNS [15].

Of importance, the brain density of both GLUT1 and GLUT3 is significantly reduced in the cerebral cortex of AD patients [16]; though, GLUT3 demonstrates a more substantial reduction (by about two-fold in the hippocampi), even being corrected for concomitant synaptic and neuronal loss [17]. Taking into account a strong positive correlation between the glucose transporters expression levels and the glucose utilization rate in the brain tissue [18], GLUT3 deficit is considered a potential cause of the brain glucose metabolism deficits associated with AD [17].

Growing evidence points to insulin resistance implication in Tau phosphorylation and consequent aggregation [19, 20]. Tau protein is soluble in its native conformation, which is essential for microtubule stabilization and axonal growth. Though, hyperphosphorylated protein tends to aggregate. This process leads to functional abnormalities, eventuates in neurodegeneration and neuronal loss. Schubert et al. (2004) designed an elegant experiment in neuron-specific IR knockout mice to demonstrate that the lack of brain insulin signaling causes Tau hyperphosphorylation [21]. Moreover, the authors confirmed the IR-mediated apparent antiapoptotic effect in neurons, shown earlier by other groups [22].

Remarkably, the semi-essential amino acid, Arginine, promotes insulin secretion in cellular models, mice, and humans [23–25]. Accordingly, several groups have proposed that Arginine relieves type 2 diabetes symptoms [26]. Peters et al. (2013) demonstrated that the enzyme that converts Arginine into Ornithine-arginase-is constitutively expressed in brain neurons [27]. Moreover, it is overactivated in the AD patients and animal models brains, which causes severe Arginine deprivation. Therefore, arginase inhibition is a promising AD-modifying strategy.

Previously, we slow-released Arginine intracerebroventricularly in a 3 × Tg mouse model of AD and demonstrated a significant improvement in spatial memory [28]. Additionally, our laboratory performed a series of experiments to study the effect of arginase inhibition with Norvaline upon AD pathogenesis [29]. This manipulation led to improvement in Arginine bioavailability and was suggested to interfere with AD pathogenesis [30]. We utilized advanced proteomics and immunohistochemistry approaches to decipher the AD molecular mechanisms and interpret our results [31, 32].

Here, we apply an advanced bioinformatics tool and analyze the integrated data from different assays. Moreover, we investigate the Tau pathology in the context of insulin signaling to close the gap in understanding the biological effects of Norvaline in the brain. We use a next-generation preclinical system for in vivo micro-PET/CT imaging and evaluate the cerebral glucose metabolism in a murine model of AD in relation to the treatment with an arginase inhibitor, Norvaline, and provide several sets of novel results uncovering its effects and molecular mechanisms of action.

Materials and Methods

Animals and Treatment

Homozygous 3 × Tg mice harboring mutant APP, PS1, and tau transgenes were obtained from Jackson Laboratory (Bar Harbor, ME) and bred in our animal facility. These animals display progressive β-amyloid (Aβ) deposition and NFT formation [33]. The mice have been treated with Norvaline in accordance with the protocol published previously [28]. Briefly, randomly chosen male 4-month-old mice were divided into four groups (3 mice in each group) and housed in individually ventilated cages. The animals were provided with water and food ad libitum. The control animals (two groups) received regular water. The experimental mice (two groups) received water with dissolved (250 mg/L) Norvaline (Sigma, St. Louis, MO, USA) for ten weeks. The experimental procedures were approved by the Bar-Ilan University animal care and use committee (approval No. 82–10-2017).

^{18}F-Fluorodeoxyglucose Positron Emission Tomography

Positron emission tomography (PET) is a well-established, reliable, non-invasive, widely used in the preclinical and clinical AD studies technique. ^{18}F-Fluorodeoxyglucose (18F-FDG) PET is a reliable imaging biomarker that allows the evaluation of cerebral glucose metabolism [34].

Here, we employed the preclinical tomography system Triumph II (TriFoil Imaging, Chatsworth, CA, USA) utilizing radiotracer fluoro-2-deoxy-2-[^{18}F]-fluoro-D-glucose (FDG-PET), to measure the brain glucose uptake. One ml of the radioactive tracer (Isotopia, Petah Tikva, Israel) has been supplied by the producer in a dose of 5 mCi (calibrated to time zero). The syringe content was transferred to a vial and diluted 1:1 with PBS. Individual syringes for each animal 200ul (± 15 MBq) have been prepared.

The control and experimental animals (three from each group) were administered with the radiotracer intraperitoneally and sedated after 40 min by inhalation of 2% isoflurane in an induction chamber [35]. Isoflurane anesthesia has been shown to have no significant effect on blood glucose levels and 18F-FDG uptake by tissues [36]. Mice were placed on the scanner warming bed, maintaining constant body temperature, secured in the prone position, and underwent micro-PET/CT scanning. The animals were kept under isoflurane anesthesia and on a heating pad during the experiment. In order to have an anatomical reference, a computed tomography (CT) imaging with 500 projections was performed. Subsequently, mice underwent a 30 min static 18F-FDG PET scan.

Image Processing

First, the original piece of software, VivoQuant™ (Invicro, New Haven, CT, USA), was used to preprocess and view the acquired images. The list-mode data were reconstructed using maximum likelihood expectation maximization (MLEM) with 20 iterations after random and scatter corrections. Activity values were normalized for the 18F-FDG dose and the animals' weights and expressed in standard uptake values (SUVs) [37]. Further processing was performed with Imaris (version 9.3, Bitplane, Zurich, Switzerland).

The raw data files were converted into IMS format with Imaris File Converter tool. The brain PET images of each mouse were spatially co-registered with their individual CT images, and 3D model has been created (Fig. 1a). Three-dimensional images were scrutinized to identify the organs with prominent signal intensities, including the brain, heart, lungs, liver, and bladder. The whole-body intensity served as the reference signal for each animal, which reflected the total body radioactivity. The ratio between the brain and the whole-body mean intensities was calculated to evaluate the relative glucose uptake by the brain tissue.

Tissue Sampling and Western Blotting

The animals which underwent the micro-PET/-CT procedure were rapidly decapitated with scissors on the following day after a test for radioactivity. Their brains were carefully removed, and the hippocampi were dissected. The collected brain tissues were separately frozen and stored at − 80 °C.

For western blot the tissue was homogenized and treated in accordance with the previously published protocol [31]. Briefly, the samples were incubated on ice and centrifuged. The protein concentration was determined using a protein assay kit (Bio-Rad, Hercules, CA, USA). Forty µg samples were subjected to sodium dodecyl sulfate–polyacrylamide gel electrophoresis and transferred onto nitrocellulose membranes.

The membranes were incubated at 4 °C overnight with primary antibody 1:1000 dilution of GLUT3 (GeneTex, Cat No. GTX129175), Anti-Insulin Receptor alpha antibody (Abcam, ab5500) and Anti-Tau (phosphor-S396) antibody (Abcam, ab109390). Following washing with Tris-buffered saline with Tween, the membranes were incubated with LI-COR dye-conjugated secondary antibody (IRDye® 680RD; LI-COR Biosciences, Lincoln, NE, USA) for 1 h at 22 °C. The beta-actin antibody was used as a reference under the same conditions (Abcam, ab8227) at 1:5000 dilution. Membranes were scanned on the Odyssey® CLx Imager (LI-COR Biosciences).

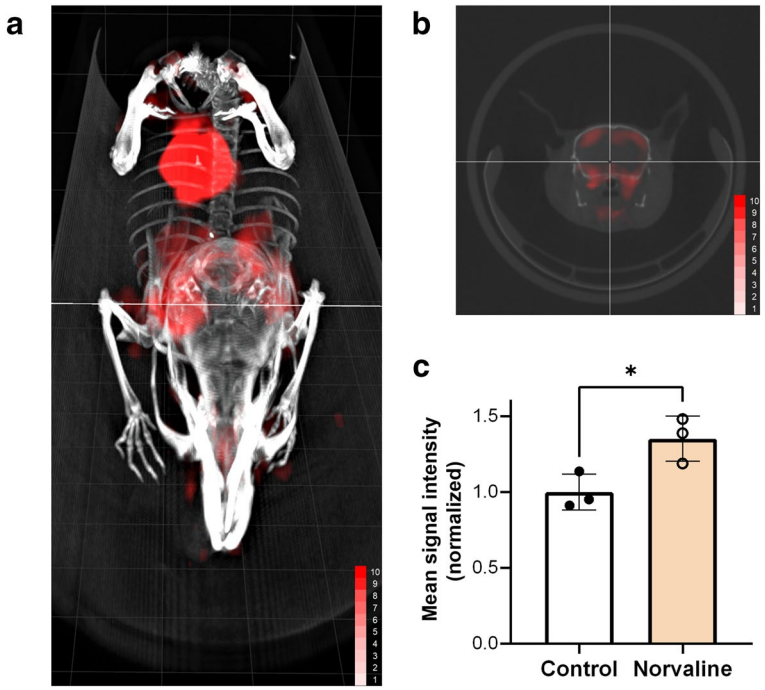

Fig. 1 FDG uptake in 3 × Tg mice. (a) Representative combined PET-CT image from the scan of Norvaline-treated 3 × Tg mouse. The image was reconstructed with Imaris. (b) 2D coronal plane of head showing solid FDG uptake by the brain. (c) Bar-chart demonstrates the treatment-dependent increase in brain glucose uptake. (n = 3, mean ± SEM, *p < 0.05)

Proteomics Data Analysis

In order to identify the molecular signatures of phenotypic state caused by treatment with Norvaline in 3 × Tg mouse brain, we performed a functional interpretation of the genes derived from two antibody microarray assays done in the previous studies [29, 32]. Earlier, we applied a stringent threshold for the lead proteins selection criteria. We analyzed only proteins that demonstrated a relatively strong net signal (≥ 750) and were up-or down-regulated by more than 45% following the treatment. Accordingly, several key for the functional characterization proteins with marginal change has been excluded from the analysis. In the present study, the combined data with more than 100 proteins and phospho-proteins (Supplementary Table S1) have been scrutinized and interpreted further.

In Silico Functional Characterization of the Leads Signature

Here, we utilized the online gene set analysis toolkit WebGestalt [38] to perform functional enrichment analysis and biological interpretation of the proteomics data. The toolkit performs the functional characterization by a gene set enrichment analysis in several databases, including the Kyoto Encyclopedia of Genes and Genomes (KEGG) [39]. Given a KEGG pathway and a reference set (such as the complete mouse genome), the ORA enrichment method we chose is based on the comparison between the fraction of signature genes in the pathway and the fraction of pathway genes in the reference set. The signature is enriched in a KEGG pathway if the former is larger than the latter fraction. To perform the enrichment analysis in KEGG, we selected the WebGestalt mouse protein-coding genome as the reference set, p-value ≤ 0.05 as the level of significance, the Benjamini–Hochberg correction to correct for multiple hypotheses.

For Fig. 1b, we selected 18 pathways among the 127 KEGG pathways found enriched in the *in-silico* functional analysis. Successively using the STRING tool, we obtained a protein–protein interactions (PPI) network table for each pathway of this selection. All these eighteen PPI tables were loaded and unified within the Cytoscape tool (Ver. 3.8) obtaining a PPI network of 35 nodes and 118 edges.

Tissue Preparation and Slicing

Six animals from the second set (three from control and three from the experimental group) were deeply anesthetized with an intraperitoneal injection of Pental (0.2 mL; CTS Chemical Industries Ltd., Kiryat Malachi, Israel) and transcardially perfused with 30 mL of PBS, followed by 50 mL of chilled 4% paraformaldehyde in PBS. The brains were removed and fixed in 4% paraformaldehyde for 24 h and then transferred to 70% ethanol at 4 °C for 48 h, dehydrated, and paraffin-embedded. The paraffin-embedded blocks were ice-cooled and sliced at a thickness of 6 µm. The sections were mounted, dried overnight at room temperature, and stored at 4 °C.

Quantitative Immunohistochemistry

Coronal hippocampal sections were immunolabeled to reveal the levels and location of a list of the proteins of interest. Staining was performed on a Leica Bond III system (Leica Biosystems Newcastle Ltd., Newcastle upon Tyne, UK). The tissues pretreated with an epitope-retrieval solution (Leica Biosystems Newcastle Ltd.) were incubated with anti-Tau (phosphor-S396) antibody (1:2000, Abcam, ab109390), and anti-BCAT1 antibody (1:400, Bioss, bs6613) for 30 min in accordance with our previously published protocol [31]. A Leica Refine-HRP kit (Leica Biosystems Newcastle Ltd.) served for hematoxylin counterstaining.

Imaging and Quantification

The brain sections were viewed under an automated upright slide scanning microscope Axio Scan.Z1 (Zeiss, Oberkochen, Germany). The images were captured with 20×/0.8 and 40×/0.95 objectives at z-planes of 0.5 µm.

Image analysis was carried out using ZEN Blue 2.5 (Zeiss) and Image-Pro Plus (Media Cybernetics). A fixed background intensity threshold was set for all sections representing a single type of staining. The images' entire z-series were deconvoluted with Huygens (Scientific Volume Imaging, Hilversum, Netherlands) to create high-resolution data. A computer-driven analysis was performed at each of the counting frame locations.

The surface of the immunoreactive area above the preset threshold was subjected to the analysis. The image densitometry method was applied to quantify the amount of staining in the specimens. The mean stain intensity of the specific channel was measured and presented as the average value for each treatment group.

Results

Norvaline Improves the Glucose Uptake by the Brain Tissue

Several sets of data indicated the effects of Norvaline upon insulin signaling and brain glucose metabolism. Accordingly, we aimed to functionally assess the treatment-related changes in the brain glucose uptake. For this purpose, we utilized PET methodology with a radioactive glucose tracer. Structural imaging using CT scanning allowed the analysis and adjustment of anatomical data. Fusion of PET and CT images with Imaris allowed accurate alignment and overlay of the common coordinate frames for each modality (Fig. 1a). The signal intensity reflected the actual radioactivity and the uptake of the tracer by tissues. Two-dimensional images (Fig. 1b) were taken to check the coordinates and compare the intensities of the signal. Finally, the normalized signals were analyzed statistically and plotted (Fig. 1c). The Student's t-test revealed a significant ($p = 0.033$, $t = 3.194$, $df = 4$) increase by 35,3% in glucose uptake by the brain tissue following the treatment with Norvaline. Remarkably, the liver demonstrated a signal similar to the brain intensity; however, the bladder, which progressively accumulated the radioactive tracer, showed the strongest signal (Fig. 1a). Of note, despite a small sample size, the data passed the Shapiro–Wilk test for normality.

Of note, the treatment did not cause significant changes in the animals' weights (Fig. S1). We observed only marginal decline and repeated measures ANOVA did not detect a significant difference between the experimental groups.

Treatment with Norvaline Affects Insulin Signaling in the Brain of AD Mice

Earlier, we implemented a series of innovative phosphoproteomics assays to examine the effects of Norvaline in the brain of AD mice. The expression levels of more than 1500 proteins have been evaluated with advanced antibody arrays in relation to the treatment applied. We have published the results with an average normalized net signal ≥ 750 and change from control $\geq 45\%$ [29, 32]. Consequently, some proteins showing high signal and relatively high treatment-related change in expression levels have not been included in the analysis.

Here, we aimed to characterize the biological pathways, validate the key leads, and evaluate the functional effects of the treatment in AD mouse brain via different methods. In the present study, we combined the data from two assays to better operate in silico functional characterization with WebGestalt tool. The analysis revealed 127 pathways significantly enriched in our signature and among them we selected the 18 most significant biological pathways, which are critically relevant to AD pathogenesis and prognosis (Fig. 2a).

In order to uncover the biological processes at the system-level and reveal possible interactions among the leads, we built protein–protein interaction (PPI) networks for each pathway shown in (Fig. 2a) with the STRING tool. The resulting unified PPI network is shown in (Fig. 2b). The analysis underlines the role of several leads within apoptosis, mTOR, and insulin signaling pathways. Of importance, the most shared leads among these three pathways are upregulated proteins based upon our proteomics experiments (supplementary Table S1). In particular, the leads in orange color (i.e., Map2k1, Akt1, and PdPk1) are shared among all these three pathways, and Akt1 represents the only leads to be downregulated. Together with Akt1, also Rps6ka1 and Igf1r are down-regulated and are all enclosed in the mTOR signaling pathway while Akt1 is the only down-regulated gene enclosed in the insulin signaling and apoptosis pathway.

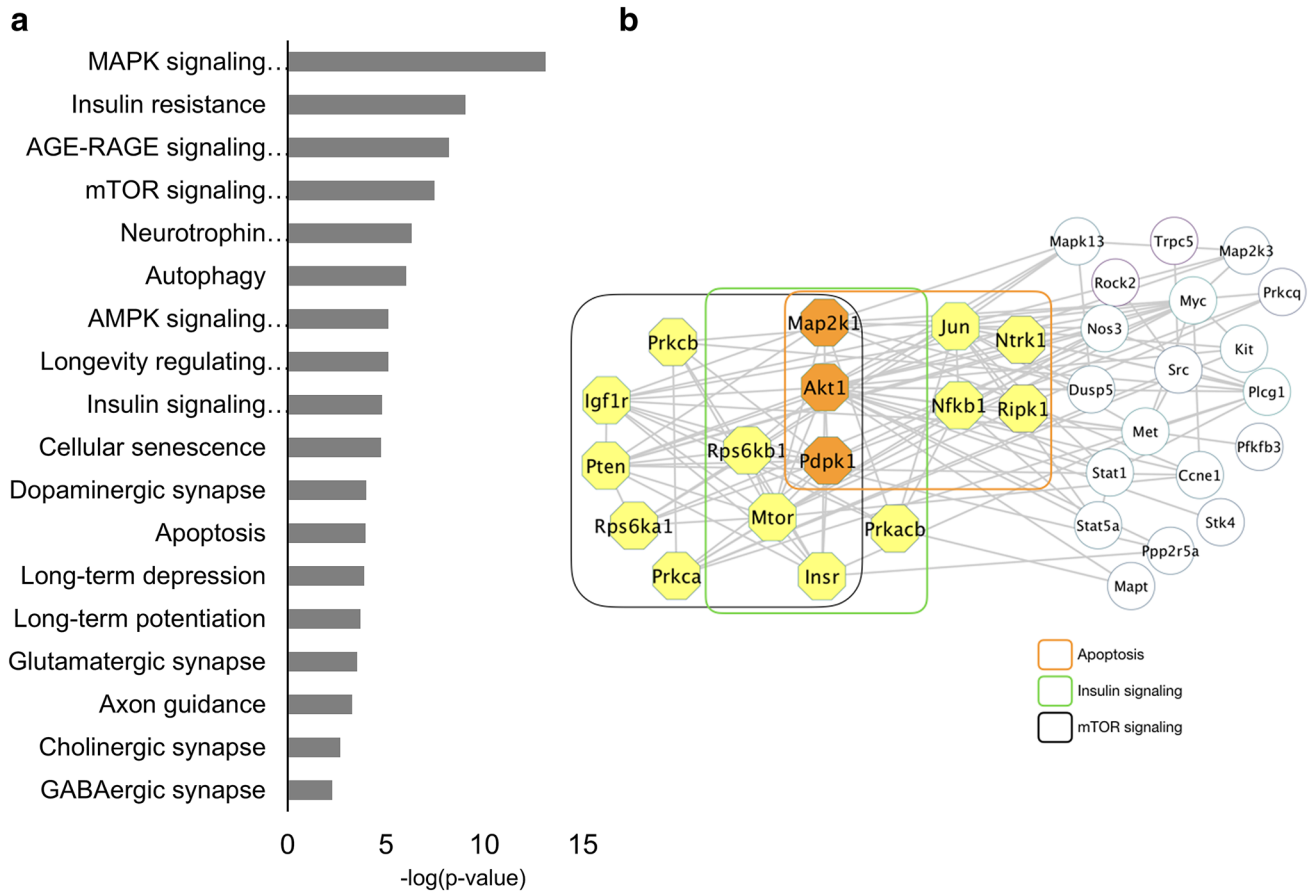

Fig. 2 Biological processes affected by norvaline treatment. (a) Enrichment analysis of KEGG pathways. WebGestalt mouse protein-coding genome served as a reference. Significantly up and down-regulated genes have been included in the analysis. (b) Cytoscape representation of the STRING protein–protein interaction map. In this network of proteins with significantly regulated phosphorylation sites detected in the proteomics assays, we focused on the proteins (yellow) involved in three most relevant KEGG pathways: apoptosis, insulin signaling, and mTOR signaling

Insulin and mTOR signaling pathways share seven significantly up- and down-regulated proteins in our analysis, highlighting their mutual involvement and interaction leading to the phenotype observed. Of note, the antibody microarray revealed no changes in the levels of Insulin-like Growth Factor 1 receptor protein-tyrosine kinase (IGF1R) (Table S1). Consequently, we suggest a critical role for alternative insulin target, namely insulin receptor, which demonstrated substantially elevated levels.

Norvaline Escalates the Expression Levels of Insulin Receptor and GLUT3 in the Hippocampus of 3 × Tg Mice

The levels of IR tested with pan-specific polyclonal antibody NK079-2 (Kinexus) demonstrated a 50% increase following the treatment. Though, it did not pass the strict 750 net signal cut-off (with a marginal index of 706) (Supplementary Table S1) and was excluded from the previous analyses.

Here, we validate this result via traditional western blotting with a different antibody. Our assay proves a significant ($p = 0.025$, $t = 3.503$, $df = 4$) treatment-associated increase (by 48.1%) in IR protein levels in the 3 × Tg mice hippocampi (Fig. 3a, b), which accords with and confirms the proteomics data.

In addition, we examined the levels of GLUT3 transporter, which shows substantially reduced levels in AD patients and 3 × Tg mice compared to wild-type animals; however, it has been proven to be treatment-sensitive [35]. Here, we evidence a significant ($p = 0.032$, $t = 3.238$, $df = 4$) 45.9% increase in GLUT3 levels following the treatment with Norvaline (Fig. 3c, d), which harmonizes with IR levels elevation.

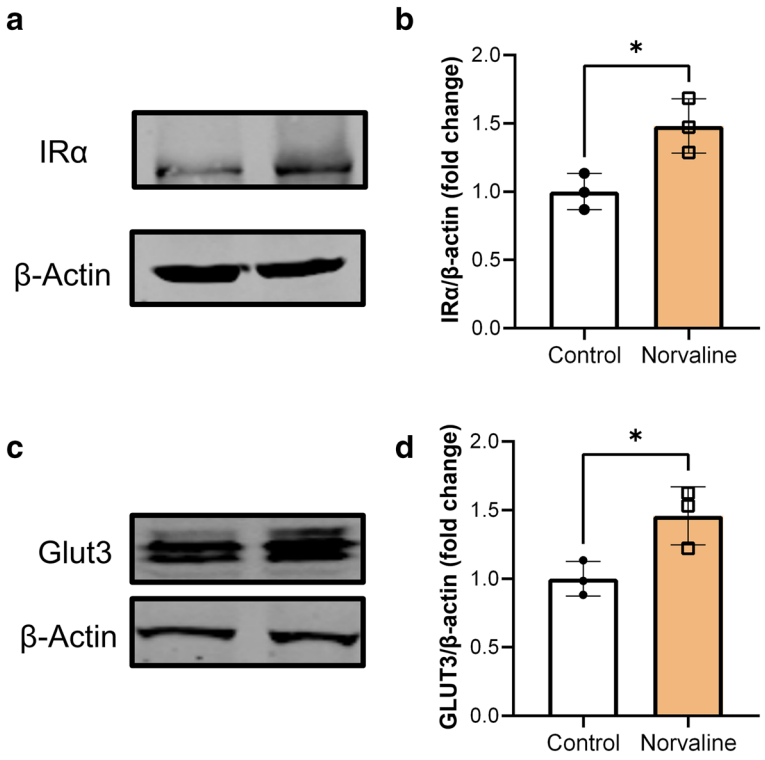

Fig. 3 Norvaline escalates the levels of insulin receptor (IR) and glucose transporter 3 (GLUT3). The hippocampal levels of IR α-subunit (IRα) and GLUT3 from 3 × Tg mice were determined by western blot analyses. Left panels (a, c) show representative western blot images of IRα, GLUT3, and β-actin (loading control). Bar graphs on the right panels (b, d) show the average IRα or GLUT3 values after normalization with the loading control and the error bars indicating ± SEM, n = 3, *p < 0.05

Norvaline Diminishes the Rate of Tau Phosphorylation at Several Functionally Critical Sites

As we have mentioned, in our previous proteomics analyses we did not report the leads showing marginal or insignificant changes in expression levels or with low signals. Accordingly, several targets related to our current subject have not been studied. Remarkably, the levels of non-phosphorylated Tau did not show a significant change (p = 0.64) following norvaline treatment with only marginal reduction by 11% (Table S1). However, Tau phosphorylated at Threonine-522 demonstrated a substantial (by 44%) reduction in levels (Table S1). Of note, T552 belongs to Tau proline-rich domain [40], which is critical for association of Tau with actin [41]. Furthermore, modifications in the proline-rich region are sufficient to induce the functional deficiencies observed in AD; and its phosphorylation plays a key role in mediating Tau-related changes [42]. Therefore, we hypothesized that Norvaline diminishes the rate of Tau phosphorylation in the brain.

In order to test this hypothesis empirically, we investigated the expression levels of another phospho-protein, Tau S396, that is commonly studied in 3 × Tg mice [43]. There are reports showing that Tau phosphorylation at S396 is one of the earliest events in AD pathology [44]. Of importance, S396 belongs to the c-terminal region, which is essential for paired helical filament formation associated with AD pathology [45].

We applied two basic molecular biology methods to assess its hippocampal levels. Western blotting of hippocampal lysates (Fig. 4c) revealed a significant (p = 0.0009, t = 8.911, df = 4) 43.75% reduction in levels of pTau following the treatment (Fig. 4d), which accords with the proteomics results. Of note, despite a small sample size (n = 3), the data passed the Shapiro–Wilk normality test.

Additionally, we stained the brains with anti-pTau antibody to characterize the spatial patterns of expression in the AD mice hippocampi (Fig. 4a). The applied statistical analysis revealed a significant (p = 0.043, t = 2.925, df = 4) effect of the treatment upon pTau immuno-positive area in the CA1 hippocampal region (Fig. 4b). Image-Pro software detected 8.7% S396-positive area in the treated group (Fig. 4a low panel), in contrast to 17.4% in the control group (Fig. 4a top panel).

Branched Chain Amino Acid Transaminase 1 (BCAT1) is Highly Expressed in the Glial and Endothelial Cells

Li et al. (2018) studied the same rodent model of AD and reported a significant down-regulation of BCAT1 in the brain tissues of 3 × Tg mice compared to wild-type animals [43]. Norvaline is an isoform of the branched chain amino acid (BCAA), Valine, and a substrate for BCAT1.

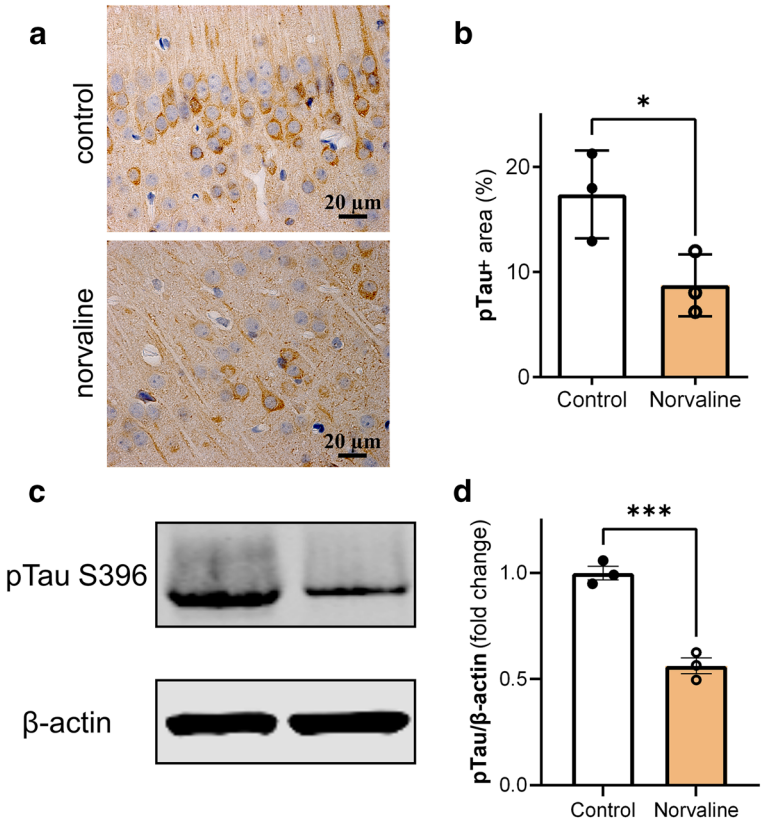

Fig. 4 Norvaline reduces the levels of pTau S396 in the hippocampi of 3×Tg mice. Representative×20 photomicrographs (a) and quantification (b) of S396 pTau-positive lesions. Representative Western blot (c) and quantitative results (d) showing the treatment-associated decrease in the levels of phosphorylated Tau protein in the hippocampi of AD mice (n = 3). ***p < 0.001, *p < 0.05 by unpaired Student's t-test

Earlier, we suggested a role of BCAA in the pathogenesis of AD and demonstrated a strong BCAT1 immunopositivity in the glial cells of C57BL/6J mice hippocampus [46]. In the present study, we stained the brains of 3×Tg mice with an anti-BCAT1 antibody to investigate the patterns of its expression in AD mice in relation to the treatment with Norvaline (Fig. 5). Of note, Norvaline is a preferred substrate for BCAT1 [47] and may affect the levels of its expression [46].

The hippocampi of 3×Tg mice have been scrutinized. The detailed analysis of the stain intensities and immunopositive areas in various brain regions did not reveal significant differences between the experimental groups (data not shown). It is noteworthy that glial cells and endothelial cells (Fig. 5 insets) demonstrate high BCAT1 immunopositivity, which accords with our previous results acquired in wild-type animals [46].

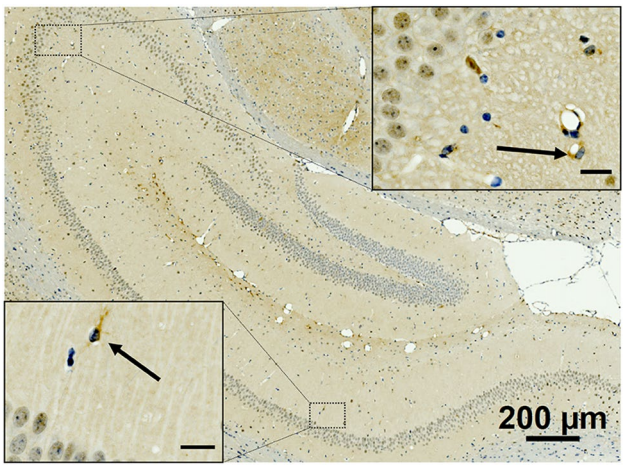

Fig. 5 Immunolocalization of cytosolic branched-chain aminotransferase (BCAT1) in the 3×Tg mouse brain. BCAT1 and hematoxylin staining of paraffin-embedded brain tissues. A representative hippocampal bright-field 20×micrograph with an inset at 40×magnification indicating expression of BCAT1 in the neurons, glial and endothelial cells (arrows). The insets scale bars are 20 µm

Discussion

The AD clinical manifestation coincides with a gradual development of typical histopathological attributes; however, they poorly correlate [48]. Accumulating evidence indicates the early appearance of metabolic abnormalities apparent at systemic, histological, and biochemical levels. Besides the distinct hallmarks, such as NFT, dystrophic neurites, and Aβ deposits, the AD-related pathology includes chronic oxidative stress, apoptosis, DNA damage, mitochondrial malfunction, and compromised energy metabolism [3].

Of importance, functional PET tests with radioactive glucose are consistently superior indicators of cognitive performances compared to scans assessing brain Aβ burden [49]. Accordingly, the causal role of amyloid plaques and NFT in the pathogenesis of AD has been repeatedly questioned [50, 51]. We believe that several factors can lead to clinical dementia with characteristic for AD hallmarks. Hence, we comprehend AD as a spectrum of pathologies with oxidative stress due to brain hypoperfusion, metabolic dysfunction, trauma, infections, etc., as a common denominator. Amyloid precursor protein overexpression or overprocessing and mutations in the Tau gene, in the cases of familial AD, also burden the brain with oxidative stress and eventuate in cognitive malfunction.

FDG-PET has been used in various animal AD models. The 5×FAD mice demonstrate significantly reduced brain glucose uptake from the age of two months compared to wild-type controls [52]. Tg4–42 mice show an apparent reduction in glucose metabolism from the age of three months [53]. Of note, the 3×Tg mice utilized here evidently demonstrate a decline in glucose brain uptake at the age of six months [35]. Remarkably, this index is proved to be treatment-sensitive. Four weeks of treatment with lipoic acid are sufficient to improve the brain glucose uptake in this murine AD model and reverse it to the wild-type animals' levels [35]. In addition, lipoic acid reverses brain symptoms of acute ischemic shock and regulates arginase expression[54].

In general, natural antioxidants such as lipoic acid [55] and ascorbic acid [56] increase glucose uptake by the tissues and improve sensitivity to insulin in diabetic patients. In the past, we have shown that the arginase inhibitors punicalagin and quercetin, reduce glucose and lipid plasma levels in obese mice [57]. Therefore, the use of such agents, potentially reducing the severity of oxidative stress in the brain [58], looks very promising. In this context, quercetin and punicalagin could also mimic Norvaline, which downregulates polyamine oxidation via arginase inhibition and represents a practical approach [51].

Here, we applied glucose uptake measures to a rodent animal AD model with the goal of tracking treatment-associated changes. Of note, FDG radiography has been previously used to assess glucose uptake by the brain tissue in 3×Tg mice [35, 59]. The present study aimed at investigating the effects of a non-competitive arginase inhibitor, Norvaline, upon the brain function in 3×Tg mice. Here, we particularly addressed the phenomenon of severe metabolic dysfunction and reduced arginine bioavailability concurring with the unfolding of typical AD symptoms. We evidence a significant effect of the treatment on the brain glucose uptake (Fig. 1) and provide an insight into the molecular mechanisms responsible for this phenomenon.

Our bioinformatics analysis demonstrated a significant effect of the treatment upon insulin and mTOR signaling in the AD mouse brain (Fig. 2). Of note, mTOR and insulin signaling are intimately interrelated. Insulin binds to IR and type 1 insulin-like growth factor receptor (IGF-1R) to evoke a series of signaling events (Fig. 6). mTOR controls insulin signaling by regulating several downstream proteins, including insulin receptor substrate-1 (IRS1) [10]. mTORC1 is a kinase that inhibits IRS1 via ribosomal S6 kinase-1 (S6K1), which phosphorylates serine residues at IRS1 and accelerates its degradation.

mTOR efficiently phosphorylates Tau protein [60], and the mTOR inhibitor, Rapamycin, attenuates the progression of Tau pathology in mice [61]. A downstream mTOR immediate effector, the cytoplasmic isoform of ribosomal S6K1 (70-kDa S6 kinase (p70S6K)), is a kinase that phosphorylates the 40S ribosomal protein S6 and plays a central role in cell growth and differentiation. Of importance, S6 protein is a substrate for both p90 and p70RSK; however, several other substrates have been identified, including Tau protein. p70S6K directly and efficiently phosphorylates Tau at several Serine and Threonine residues [62]. Remarkably, reducing S6K1 expression diminishes Tau pathology, improves spatial memory and synaptic plasticity in 3×Tg mice [63]. In our study, treatment with Norvaline led to histological changes, which are very similar to the results from the quoted above paper. In this context, it is worth noting that Norvaline is a potent inhibitor of S6K1 [64]. Thus, the observed Tau-related phenotype (Fig. 4) is explicable; though, the precise mechanism is unclear. Hence, we addressed the question of mTOR and S6K1 activity in our proteomics assays.

Of note, ERK-dependent phosphorylation of p90 ribosomal protein S6 kinase RSK1 at S352 is crucial for its activation [65]. We evidenced a substantial (90%) reduction in the levels of this phosphoprotein (Table S1). Additionally, treatment with Norvaline led to a 55% increase in levels of PTEN, which is a negative regulator of IRS2. PTEN also upregulates the interaction between IRS2 and PI3K [66].

Surprisingly, the levels of mTOR protein increased (by 66%) following the treatment with Norvaline (Table S1). Moreover, the levels of mTOR active form, phosphorylated at S2481, upsurged by 112%. This phenomenon reflects the dualistic pattern of Norvaline effects in the brain. This non-proteinogenic amino acid evidently upregulates the insulin pathway but silences several downstream enzymes responsible for the negative feedback mechanism.

In general, BCAA (leucine, isoleucine, and valine) are potent activators of the mTOR pathway [67]. Leucine supplement promotes mTOR signaling activation in vitro and in the brains of AD mice [43]. Moreover, leucine significantly increases the rate of Tau phosphorylation in these models. Norvaline competes with BCAA for the same transport routes [46]. Then, its supplement affects the intracellular

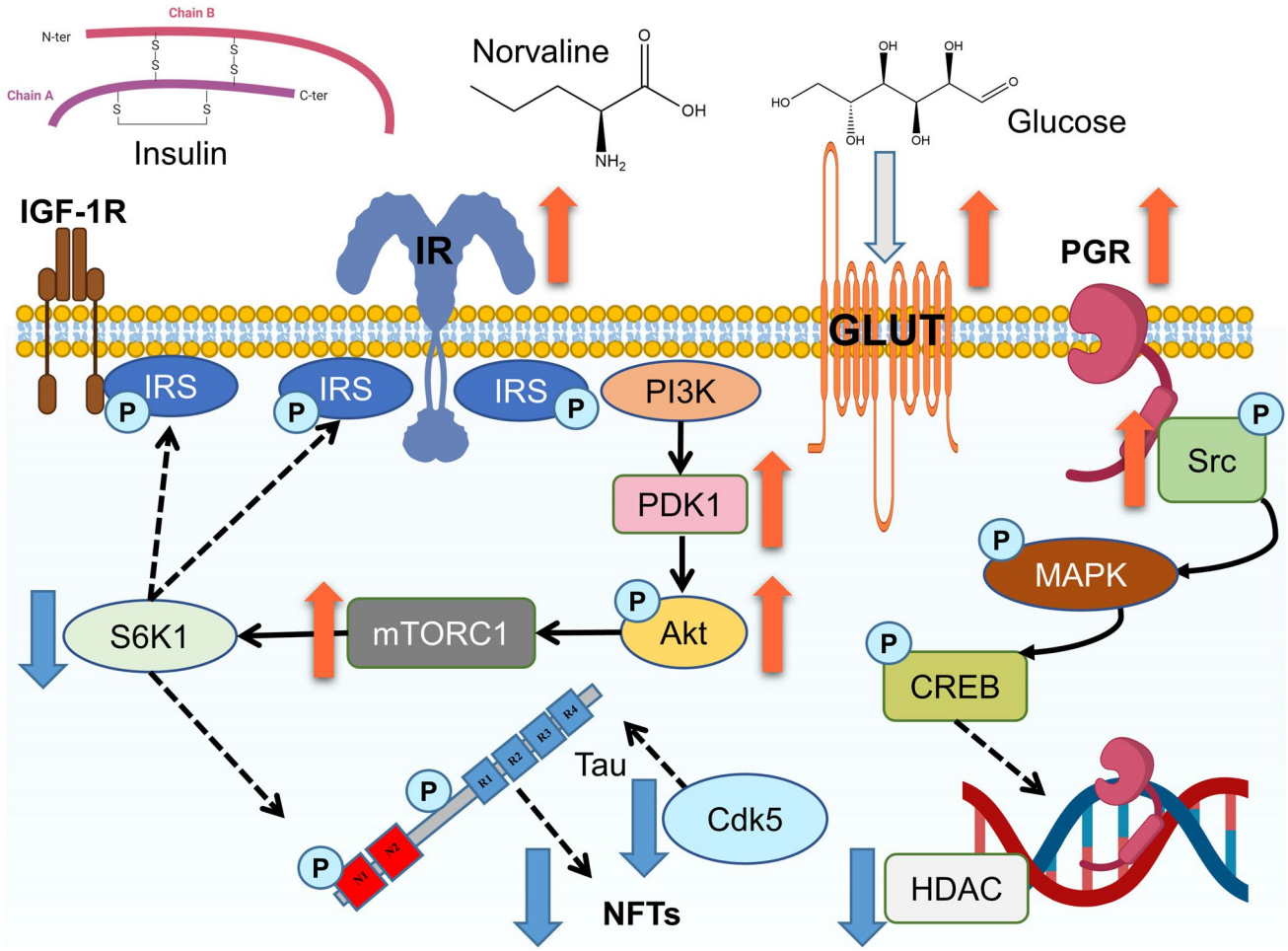

Fig. 6 Hypothetical model of the Norvaline sites of action and effects upon 3×Tg mouse brain glucose metabolism. The cartoon depicts several biological pathways affected by Norvaline and involved in glucose uptake, GLUT3 expression, IR expression and activity, and Tau phosphorylation. Ligand binding to IR initiates metabolic signaling with cascade activation of downstream effectors. IR and IGF-1R are tyrosine kinases that activate insulin receptor substrate (IRS) via Tyrosine residues phosphorylation, which activates downstream peptides including mTORC1. RAC-alpha serine/threonine-protein kinase (AKT) mediates most of insulin's metabolic effects (glucose transport, lipid synthesis, gluconeogenesis, and glycogen synthesis). This kinase plays a central role in the control of cell cycle and survival. mTORC1 and S6K1 are kinases that phosphorylate Serine residues at IRS1, which causes its degradation. In addition, mTOR and S6K1 phosphorylate Tau at multiple sites, which causes its aggregation. RAC-alpha serine/threonine-protein kinase (AKT), Insulin-like Growth Factor 1 receptor (IGF1R), Insulin Receptor (IR) Progesterone Receptor (PGR), Phosphoinositide 3-Kinase (PI3K), 3-Phosphoinositide-Dependent Kinase-1 (PDK1), Cyclin-Dependent protein-serine kinase 5 (Cdk5), mitogen-activated protein kinase (MAPK), cAMP-response Element-Binding protein (CREB), Mechanistic Target of Rapamycin Complex 1 (mTORC1), Histone Deacetylase (HDAC), proto-oncogene tyrosine-protein kinase Src (Src), ribosomal S6 kinase-1 (S6K1), Neurofibrillary Tangles (NFTs)

concentrations of other amino acids, which potentially influences the activity of mTOR.

Remarkably, treatment with Norvaline led to substantial changes in expression levels of other proteins that affect glucose metabolism and Tau phosphorylation (Table S1). Earlier, we evidenced a significant (65%) decrease in levels of functionally active (phosphorylated at S498) form of histone deacetylase 5 (HDAC5) [32]. HDAC5 has been proven to regulate glucose uptake and insulin action in mammals. McGee et al. (2008) have established that HDAC5 represses the GLUT4 gene [68]. Another group showed that HDAC5 knockdown increases glucose uptake and GLUT4 expression in muscle cells [69]. Of note, HDAC5 regulates histone acetylation and plays a central role in various brain disorders' pathogenesis. Its targeting has been proposed as a promising AD-modifying therapy [70]. Consequently, several HDAC5 inhibitors have been suggested as efficient therapeutic agents [71].

Cyclin-dependent protein-serine kinase 5 (Cdk5) pY15 demonstrated even more substantial decline in levels (by 85%) following the treatment (Table S1). Cdk5 overactivation has been linked to AD-associated neurodegeneration

[72], and Cdk5 inhibition has been suggested as a promising neurodegeneration treatment strategy [73]. Of note, Cdk5 is the key factor in Tau aggregation and NFT formation [74]. Saito et al. (2019) elegantly proved the role of Cdk5 in pathological Tau accumulation and toxicity [75]. Additionally, Cdk5 was shown to regulate glucose-stimulated insulin secretion. Its inhibition improves the inward whole-cell Ca^{2+} channel current and enhances insulin secretion [76].

Recent evidence points to progesterone neuroprotective properties, particularly in the context of AD. Wu et al. (2019) treated AD mice with progesterone for 40 days to show significantly escalated (by more than 100%) expression levels of GLUT3 and GLUT4 in the brain, accompanied by an improvement in learning and memory [77]. *In-vitro* study with cortical neurons proved a significant effect of progesterone on glucose uptake by promoting the expression of GLUT3 and GLUT4. Earlier, another group demonstrated that progesterone treatment induces the accumulation of GLUT3 and possesses neuroprotective properties during a hypoxic-ischemic injury in a cerebral ischemic rodent model [78].

In order to execute its biological effects in the brain, progesterone binds to an array of receptors (PGRs), including the nuclear receptor, which acts as a transcription factor, thus inducing a series of downstream events. The constant expression of PGN at the cellular membrane is ensured by the dynamic nucleo-cytoplasmic shuttle mechanism [79]. Progesterone binding induces the association of PGR and proto-oncogene tyrosine-protein kinase Src (Src) and leads to activation of the MAPK module (Fig. 6) [80].

Remarkably, our assay disclosed a substantial (47%) treatment-associated increase in the levels of progesterone receptor (PGR) in the hippocampi of 3 × Tg mice (Table S1). Additionally, we show a spectacular upsurge (by 924%) in the levels of active Src form phosphorylated at Y419, which indicates PGR activation. These findings provide a clue to the understanding of the treatment-associated GLUT3 upregulation (Fig. 3c).

We also disclose a substantial (by 426%) increase in levels of 3-phosphoinositide-dependent protein kinase-1 (PDPK1) (Table S1). PDK1 is a master kinase that is crucial for the activation of the AKT pathway (Fig. 6). Of note, PDPK1 is a universal effector activated by several growth factors and hormones, including insulin.

Finally, we verified the treatment-associated elevation in the levels of IR (Table S1) via traditional western blot (Fig. 3a). These findings accord with the results published by Sancheti et al. (2013), who showed the effect of feeding with lipoic acid on the levels of GLUT3 and insulin signaling in the brains of 3 × Tg mice [35]. Of note, most of insulin's metabolic effects, including glucose transport, lipid synthesis, gluconeogenesis, and glycogen synthesis, are mediated via RAC (Rho family)-alpha serine/threonine-protein kinase (AKT) [81]. AKT also plays a role in the control of cell cycle and survival. Our assay demonstrates an increase (by 135%) in the levels of this kinase phosphorylated at Y326 (Table S1) following the treatment with Norvaline, which further indicates the treatment-associated improvement in insulin signaling.

There is a consensus in the current literature on the pivotal role of glucose metabolism malfunction in AD pathogenesis. This abnormality induces mitochondrial dysfunction and leads to oxidative stress. Evidently, several factors cause cerebral hypometabolism, which eventuates in typical AD clinical and histological profiles. Though, glucose uptake measures with FDG-microPET is an ideal non-invasive diagnostic tool and biomarker for early AD diagnosis and testing of novel disease-modifying interventions. In this context, we highlight that arginase inhibition demonstrates a wide-ranging therapeutic potential. Being an isoform of BCAA Valine, Norvaline possesses multidimensional modes of activity interfering with several aspects of AD and diabetes mellitus pathogenesis. Then, it is a promising candidate for further examination.

Conclusions

Insulin action in the healthy brain and its role in the pathogenesis of neurodegenerative diseases represent a novel research frontier. Several critical questions are still open. In particular, the precise transport mechanism via which the peripheral insulin reaches the CNS and the relative role of locally synthesized in the brain hormone in different physiologic and pathologic conditions are topics for future investigations.

In relation to AD, it is critical to unravel the Gordian knot of causal relationships between the neuropathological hallmarks and clinical dementia manifestation to pave a road to efficient disease-modifying treatments. AD is an extremely complex pathology with uncertain etiology and indefinite onset. This idiosyncrasy significantly complicates the studies and halts the development of an efficient disease-modifying treatment strategy.

In closing, we admit that our experimental design and setting are not optimal and suffer from methodological and technical limitations. Still, the present study substantially improves the current knowledge on insulin function in the brain and explicates the link between insulin signaling and Tau pathology at molecular and cellular levels.

Supplementary Information The online version contains supplementary material available at https://doi.org/10.1007/s11064-021-03519-3.

Acknowledgements We gratefully acknowledge Dr. Zohar Gavish for his help with immunohistochemistry.

Author Contributions BP and AS designed the experiments. BP was involved in all the aspects of the work and wrote the manuscript. KDS assisted in tissue sampling, western blot, immunohistochemistry, and initial data analysis. MS assisted in conducting the in-silico part. VG assisted in PET-CT experiments and statistical analysis. MA assisted in data analysis. AOS conceived, designed, supervised the experiments, and edited the manuscript.

Funding This research was supported by Marie Curie CIG Grant 322113, Leir Foundation Grant, Ginzburg Family Foundation Grant, and Katz Foundation Grant (all to AOS).

Data Availability The analyzed data sets generated during the study are available from the corresponding author on reasonable request.

Declarations

Conflict of interest The authors declare no conflicts of interest.

Ethical Approval The study was approved by the Bar-Ilan University Animal Care and Use Committee (approval No. 82–10-2017) on October 1, 2017.

Consent for Publication Not applicable.

References

1. 2020 Alzheimer's disease facts and figures. Alzheimers Dement. 2020. https://doi.org/10.1002/alz.12068.
2. Goedert M, Spillantini MG (2006) A century of Alzheimer's disease. Science 314(5800):777–781. https://doi.org/10.1126/science.1132814
3. Polis B, Samson AO (2019) A new perspective on Alzheimer's disease as a brain expression of a complex metabolic disorder. In: Wisniewski T (ed) Alzheimer's disease. Brisbane(AU)
4. Avitan I, Halperin Y, Saha T, Bloch N, Atrahimovich D, Polis B et al (2021) Towards a consensus on Alzheimer's disease comorbidity? J Clin Med. 10(19):10. https://doi.org/10.3390/jcm10194360
5. Mosconi L, Pupi A, De Leon MJ (2008) Brain glucose hypometabolism and oxidative stress in preclinical Alzheimer's disease. Ann N Y Acad Sci 1147:180–195. https://doi.org/10.1196/annals.1427.007
6. Minoshima S, Frey KA, Koeppe RA, Foster NL, Kuhl DE (1995) A diagnostic approach in Alzheimer's disease using three-dimensional stereotactic surface projections of fluorine-18-FDG PET. J Nucl Med 36(7):1238–1248
7. Minoshima S, Giordani B, Berent S, Frey KA, Foster NL, Kuhl DE (1997) Metabolic reduction in the posterior cingulate cortex in very early Alzheimer's disease. Ann Neurol 42(1):85–94. https://doi.org/10.1002/ana.410420114
8. Talbot K, Wang HY, Kazi H, Han LY, Bakshi KP, Stucky A et al (2012) Demonstrated brain insulin resistance in Alzheimer's disease patients is associated with IGF-1 resistance, IRS-1 dysregulation, and cognitive decline. J Clin Invest 122(4):1316–1338. https://doi.org/10.1172/JCI59903
9. de la Monte SM, Wands JR (2008) Alzheimer's disease is type 3 diabetes-evidence reviewed. J Diabetes Sci Technol 2(6):1101–1113. https://doi.org/10.1177/193229680800200619
10. Petersen MC, Shulman GI (2018) Mechanisms of insulin action and insulin resistance. Physiol Rev 98(4):2133–2223. https://doi.org/10.1152/physrev.00063.2017
11. Gray SM, Barrett EJ (2018) Insulin transport into the brain. Am J Physiol Cell Physiol 315(2):C125–C136. https://doi.org/10.1152/ajpcell.00240.2017
12. Kobayashi M, Nikami H, Morimatsu M, Saito M (1996) Expression and localization of insulin-regulatable glucose transporter (GLUT4) in rat brain. Neurosci Lett 213(2):103–106. https://doi.org/10.1016/0304-3940(96)12845-7
13. Simpson IA, Dwyer D, Malide D, Moley KH, Travis A, Vannucci SJ (2008) The facilitative glucose transporter GLUT3: 20 years of distinction. Am J Physiol Endocrinol Metab 295(2):E242–E253. https://doi.org/10.1152/ajpendo.90388.2008
14. Maher F, Simpson IA (1994) The GLUT3 glucose transporter is the predominant isoform in primary cultured neurons: assessment by biosynthetic and photoaffinity labelling. Biochem J 301(Pt 2):379–384. https://doi.org/10.1042/bj3010379
15. Maher F, Davies-Hill TM, Simpson IA (1996) Substrate specificity and kinetic parameters of GLUT3 in rat cerebellar granule neurons. Biochem J 315(Pt 3):827–831. https://doi.org/10.1042/bj3150827
16. Kyrtata N, Emsley HCA, Sparasci O, Parkes LM, Dickie BR (2021) A systematic review of glucose transport alterations in Alzheimer's disease. Front Neurosci 15:626636. https://doi.org/10.3389/fnins.2021.626636
17. Simpson IA, Chundu KR, Davies-Hill T, Honer WG, Davies P (1994) Decreased concentrations of GLUT1 and GLUT3 glucose transporters in the brains of patients with Alzheimer's disease. Ann Neurol 35(5):546–551. https://doi.org/10.1002/ana.410350507
18. Vannucci SJ, Maher F, Simpson IA (1997) Glucose transporter proteins in brain: delivery of glucose to neurons and glia. Glia 21(1):2–21. https://doi.org/10.1002/(sici)1098-1136(199709)21:1%3c2::aid-glia2%3e3.0.co;2-c
19. Lesort M, Jope RS, Johnson GV (1999) Insulin transiently increases tau phosphorylation: involvement of glycogen synthase kinase-3beta and Fyn tyrosine kinase. J Neurochem 72(2):576–584. https://doi.org/10.1046/j.1471-4159.1999.0720576.x
20. Lesort M, Johnson GV (2000) Insulin-like growth factor-1 and insulin mediate transient site-selective increases in tau phosphorylation in primary cortical neurons. Neuroscience 99(2):305–316. https://doi.org/10.1016/s0306-4522(00)00200-1
21. Schubert M, Gautam D, Surjo D, Ueki K, Baudler S, Schubert D et al (2004) Role for neuronal insulin resistance in neurodegenerative diseases. Proc Natl Acad Sci USA 101(9):3100–3105. https://doi.org/10.1073/pnas.0308724101
22. Tanaka M, Sawada M, Yoshida S, Hanaoka F, Marunouchi T (1995) Insulin prevents apoptosis of external granular layer neurons in rat cerebellar slice cultures. Neurosci Lett 199(1):37–40. https://doi.org/10.1016/0304-3940(95)12009-s
23. Umeda M, Hiramoto M, Watanabe A, Tsunoda N, Imai T (2015) Arginine-induced insulin secretion in endoplasmic reticulum. Biochem Biophys Res Commun 466(4):717–722. https://doi.org/10.1016/j.bbrc.2015.09.006
24. Thams P, Capito K (1999) L-arginine stimulation of glucose-induced insulin secretion through membrane depolarization and independent of nitric oxide. Eur J Endocrinol 140(1):87–93. https://doi.org/10.1530/eje.0.1400087
25. Leiss V, Flockerzie K, Novakovic A, Rath M, Schonsiegel A, Birnbaumer L et al (2014) Insulin secretion stimulated by L-arginine and its metabolite L-ornithine depends on Galpha(i2). Am J Physiol Endocrinol Metab 307(9):E800–E812. https://doi.org/10.1152/ajpendo.00337.2014
26. Hu S, Han M, Rezaei A, Li D, Wu G, Ma X (2017) L-Arginine modulates glucose and lipid metabolism in obesity and diabetes. Curr Protein Pept Sci 18(6):599–608. https://doi.org/10.2174/1389203717666160627074017

27. Peters D, Berger J, Langnaese K, Derst C, Madai VI, Krauss M et al (2013) Arginase and arginine decarboxylase—where do the putative gate keepers of polyamine synthesis reside in rat brain? PLoS ONE 8(6):e66735. https://doi.org/10.1371/journal.pone.0066735
28. Fonar G, Polis B, Meirson T, Maltsev A, Elliott E, Samson AO (2018) Intracerebroventricular administration of L-arginine improves spatial memory acquisition in triple transgenic mice via reduction of oxidative stress and apoptosis. Transl Neurosci 9:43–53. https://doi.org/10.1515/tnsci-2018-0009
29. Polis B, Srikanth KD, Elliott E, Gil-Henn H, Samson AO (2018) L-norvaline reverses cognitive decline and synaptic loss in a murine model of Alzheimer's Disease. Neurotherapeutics 15(4):1036–1054. https://doi.org/10.1007/s13311-018-0669-5
30. Kan MJ, Lee JE, Wilson JG, Everhart AL, Brown CM, Hoofnagle AN et al (2015) Arginine deprivation and immune suppression in a mouse model of Alzheimer's disease. J Neurosci 35(15):5969–5982. https://doi.org/10.1523/JNEUROSCI.4668-14.2015
31. Polis B, Srikanth KD, Gurevich V, Gil-Henn H, Samson AO (2019) L-Norvaline, a new therapeutic agent against Alzheimer's disease. Neural Regen Res 14(9):1562–1572. https://doi.org/10.4103/1673-5374.255980
32. Polis B, Srikanth KD, Gurevich V, Bloch N, Gil-Henn H, Samson AO (2020) Arginase inhibition supports survival and differentiation of neuronal precursors in adult Alzheimer's disease mice. Int J Mol Sci. https://doi.org/10.3390/ijms21031133
33. Oddo S, Caccamo A, Shepherd JD, Murphy MP, Golde TE, Kayed R et al (2003) Triple-transgenic model of Alzheimer's disease with plaques and tangles: intracellular Abeta and synaptic dysfunction. Neuron 39(3):409–421. https://doi.org/10.1016/s0896-6273(03)00434-3
34. Bouter C, Bouter Y (2019) (18)F-FDG-PET in mouse models of Alzheimer's disease. Front Med (Lausanne) 6:71. https://doi.org/10.3389/fmed.2019.00071
35. Sancheti H, Akopian G, Yin F, Brinton RD, Walsh JP, Cadenas E (2013) Age-dependent modulation of synaptic plasticity and insulin mimetic effect of lipoic acid on a mouse model of Alzheimer's disease. PLoS ONE 8(7):e69830. https://doi.org/10.1371/journal.pone.0069830
36. Fueger BJ, Czernin J, Hildebrandt I, Tran C, Halpern BS, Stout D et al (2006) Impact of animal handling on the results of 18F-FDG PET studies in mice. J Nucl Med 47(6):999–1006
37. Bellaver B, Rocha AS, Souza DG, Leffa DT, De Bastiani MA, Schu G et al (2019) Activated peripheral blood mononuclear cell mediators trigger astrocyte reactivity. Brain Behav Immun 80:879–888. https://doi.org/10.1016/j.bbi.2019.05.041
38. Wang J, Vasaikar S, Shi Z, Greer M, Zhang B (2017) WebGestalt 2017: a more comprehensive, powerful, flexible and interactive gene set enrichment analysis toolkit. Nucleic Acids Res 45(W1):W130–W137. https://doi.org/10.1093/nar/gkx356
39. Kanehisa M, Goto S (2000) KEGG: kyoto encyclopedia of genes and genomes. Nucleic Acids Res 28(1):27–30. https://doi.org/10.1093/nar/28.1.27
40. Dixit H, Kumar CS, Chaudhary R, Thaker D, Gadewal N, Dasgupta D (2021) Role of phosphorylation and hyperphosphorylation of tau in its interaction with betaalpha dimeric tubulin studied from a bioinformatics perspective. Avicenna J Med Biotechnol 13(1):24–34. https://doi.org/10.18502/ajmb.v13i1.4579
41. He HJ, Wang XS, Pan R, Wang DL, Liu MN, He RQ (2009) The proline-rich domain of tau plays a role in interactions with actin. BMC Cell Biol 10:81. https://doi.org/10.1186/1471-2121-10-81
42. Eidenmuller J, Fath T, Maas T, Pool M, Sontag E, Brandt R (2001) Phosphorylation-mimicking glutamate clusters in the proline-rich region are sufficient to simulate the functional deficiencies of hyperphosphorylated tau protein. Biochem J 357(Pt 3):759–767. https://doi.org/10.1042/0264-6021:3570759
43. Li H, Ye D, Xie W, Hua F, Yang Y, Wu J et al (2018) Defect of branched-chain amino acid metabolism promotes the development of Alzheimer's disease by targeting the mTOR signaling. Biosci Rep. https://doi.org/10.1042/BSR20180127
44. Mondragon-Rodriguez S, Perry G, Luna-Munoz J, Acevedo-Aquino MC, Williams S (2014) Phosphorylation of tau protein at sites Ser(396–404) is one of the earliest events in Alzheimer's disease and Down syndrome. Neuropathol Appl Neurobiol 40(2):121–135. https://doi.org/10.1111/nan.12084
45. Yanagawa H, Chung SH, Ogawa Y, Sato K, Shibata-Seki T, Masai J et al (1998) Protein anatomy: C-tail region of human tau protein as a crucial structural element in Alzheimer's paired helical filament formation in vitro. Biochemistry 37(7):1979–1988. https://doi.org/10.1021/bi9724265
46. Polis B, Samson AO (2020) Role of the metabolism of branched-chain amino acids in the development of Alzheimer's disease and other metabolic disorders. Neural Regen Res 15(8):1460–1470. https://doi.org/10.4103/1673-5374.274328
47. Davoodi J, Drown PM, Bledsoe RK, Wallin R, Reinhart GD, Hutson SM (1998) Overexpression and characterization of the human mitochondrial and cytosolic branched-chain aminotransferases. J Biol Chem 273(9):4982–4989. https://doi.org/10.1074/jbc.273.9.4982
48. Serrano-Pozo A, Qian J, Muzikansky A, Monsell SE, Montine TJ, Frosch MP et al (2016) Thal amyloid stages do not significantly impact the correlation between neuropathological change and cognition in the Alzheimer disease continuum. J Neuropathol Exp Neurol 75(6):516–526. https://doi.org/10.1093/jnen/nlw026
49. Khosravi M, Peter J, Wintering NA, Serruya M, Shamchi SP, Werner TJ et al (2019) 18F-FDG is a superior indicator of cognitive performance compared to 18F-Florbetapir in Alzheimer's disease and mild cognitive impairment evaluation: a global quantitative analysis. J Alzheimers Dis 70(4):1197–1207. https://doi.org/10.3233/JAD-190220
50. Lee HG, Castellani RJ, Zhu X, Perry G, Smith MA (2005) Amyloid-beta in Alzheimer's disease: the horse or the cart? Pathogenic or protective? Int J Exp Pathol 86(3):133–138. https://doi.org/10.1111/j.0959-9673.2005.00429.x
51. Polis B, Karasik D, Samson AO (2021) Alzheimer's disease as a chronic maladaptive polyamine stress response. Aging (Albany NY) 13(7):10770–10795. https://doi.org/10.18632/aging.202928
52. Macdonald IR, DeBay DR, Reid GA, O'Leary TP, Jollymore CT, Mawko G et al (2014) Early detection of cerebral glucose uptake changes in the 5XFAD mouse. Curr Alzheimer Res 11(5):450–460. https://doi.org/10.2174/1567205011666140505111354
53. Bouter C, Henniges P, Franke TN, Irwin C, Sahlmann CO, Sichler ME et al (2018) (18)F-FDG-PET detects drastic changes in brain metabolism in the Tg4-42 model of Alzheimer's disease. Front Aging Neurosci 10:425. https://doi.org/10.3389/fnagi.2018.00425
54. Wang Q, Lv C, Sun Y, Han X, Wang S, Mao Z et al (2018) The role of alpha-lipoic acid in the pathomechanism of acute ischemic stroke. Cell Physiol Biochem 48(1):42–53. https://doi.org/10.1159/000491661
55. Yaworsky K, Somwar R, Ramlal T, Tritschler HJ, Klip A (2000) Engagement of the insulin-sensitive pathway in the stimulation of glucose transport by alpha-lipoic acid in 3T3-L1 adipocytes. Diabetologia 43(3):294–303. https://doi.org/10.1007/s001250050047
56. Dakhale GN, Chaudhari HV, Shrivastava M (2011) Supplementation of vitamin C reduces blood glucose and improves glycosylated hemoglobin in type 2 diabetes mellitus: a randomized, double-blind study. Adv Pharmacol Sci 2011:195271. https://doi.org/10.1155/2011/195271
57. Atrahimovich D, Samson AO, Khattib A, Vaya J, Khatib S (2018) Punicalagin decreases serum glucose levels and increases PON1 activity and HDL anti-inflammatory values in Balb/c mice fed a

high-fat diet. Oxid Med Cell Longev 2018:2673076. https://doi.org/10.1155/2018/2673076
58. Malpica-Nieves CJ, Rivera-Aponte DE, Tejeda-Bayron FA, Mayor AM, Phanstiel O, Veh RW et al (2020) The involvement of polyamine uptake and synthesis pathways in the proliferation of neonatal astrocytes. Amino Acids 52(8):1169–1180. https://doi.org/10.1007/s00726-020-02881-w
59. Nicholson RM, Kusne Y, Nowak LA, LaFerla FM, Reiman EM, Valla J (2010) Regional cerebral glucose uptake in the 3xTG model of Alzheimer's disease highlights common regional vulnerability across AD mouse models. Brain Res 1347:179–185. https://doi.org/10.1016/j.brainres.2010.05.084
60. Caccamo A, Magri A, Medina DX, Wisely EV, Lopez-Aranda MF, Silva AJ et al (2013) mTOR regulates tau phosphorylation and degradation: implications for Alzheimer's disease and other tauopathies. Aging Cell 12(3):370–380. https://doi.org/10.1111/acel.12057
61. Ozcelik S, Fraser G, Castets P, Schaeffer V, Skachokova Z, Breu K et al (2013) Rapamycin attenuates the progression of tau pathology in P301S tau transgenic mice. PLoS ONE 8(5):e62459. https://doi.org/10.1371/journal.pone.0062459
62. Pei JJ, An WL, Zhou XW, Nishimura T, Norberg J, Benedikz E et al (2006) P70 S6 kinase mediates tau phosphorylation and synthesis. FEBS Lett 580(1):107–114. https://doi.org/10.1016/j.febslet.2005.11.059
63. Caccamo A, Branca C, Talboom JS, Shaw DM, Turner D, Ma L et al (2015) Reducing Ribosomal Protein S6 Kinase 1 Expression Improves Spatial Memory and Synaptic Plasticity in a Mouse Model of Alzheimer's Disease. J Neurosci 35(41):14042–14056. https://doi.org/10.1523/JNEUROSCI.2781-15.2015
64. Ming XF, Rajapakse AG, Carvas JM, Ruffieux J, Yang Z (2009) Inhibition of S6K1 accounts partially for the anti-inflammatory effects of the arginase inhibitor L-norvaline. BMC Cardiovasc Disord 9:12. https://doi.org/10.1186/1471-2261-9-12
65. Dalby KN, Morrice N, Caudwell FB, Avruch J, Cohen P (1998) Identification of regulatory phosphorylation sites in mitogen-activated protein kinase (MAPK)-activated protein kinase-1a/p90rsk that are inducible by MAPK. J Biol Chem 273(3):1496–1505. https://doi.org/10.1074/jbc.273.3.1496
66. Simpson L, Li J, Liaw D, Hennessy I, Oliner J, Christians F et al (2001) PTEN expression causes feedback upregulation of insulin receptor substrate 2. Mol Cell Biol 21(12):3947–3958. https://doi.org/10.1128/MCB.21.12.3947-3958.2001
67. Moberg M, Apro W, Ekblom B, van Hall G, Holmberg HC, Blomstrand E (2016) Activation of mTORC1 by leucine is potentiated by branched-chain amino acids and even more so by essential amino acids following resistance exercise. Am J Physiol Cell Physiol 310(11):C874–C884. https://doi.org/10.1152/ajpcell.00374.2015
68. McGee SL, van Denderen BJ, Howlett KF, Mollica J, Schertzer JD, Kemp BE et al (2008) AMP-activated protein kinase regulates GLUT4 transcription by phosphorylating histone deacetylase 5. Diabetes 57(4):860–867. https://doi.org/10.2337/db07-0843
69. Raichur S, Teh SH, Ohwaki K, Gaur V, Long YC, Hargreaves M et al (2012) Histone deacetylase 5 regulates glucose uptake and insulin action in muscle cells. J Mol Endocrinol 49(3):203–211. https://doi.org/10.1530/JME-12-0095
70. Xu K, Dai XL, Huang HC, Jiang ZF (2011) Targeting HDACs: a promising therapy for Alzheimer's disease. Oxid Med Cell Longev 2011:143269. https://doi.org/10.1155/2011/143269
71. Yang SS, Zhang R, Wang G, Zhang YF (2017) The development prospection of HDAC inhibitors as a potential therapeutic direction in Alzheimer's disease. Transl Neurodegener 6:19. https://doi.org/10.1186/s40035-017-0089-1
72. Shah K, Lahiri DK (2014) Cdk5 activity in the brain - multiple paths of regulation. J Cell Sci 127(Pt 11):2391–2400. https://doi.org/10.1242/jcs.147553
73. Kanungo J, Zheng YL, Amin ND, Pant HC (2009) Targeting Cdk5 activity in neuronal degeneration and regeneration. Cell Mol Neurobiol 29(8):1073–1080. https://doi.org/10.1007/s10571-009-9410-6
74. Noble W, Olm V, Takata K, Casey E, Mary O, Meyerson J et al (2003) Cdk5 is a key factor in tau aggregation and tangle formation in vivo. Neuron 38(4):555–565. https://doi.org/10.1016/s0896-6273(03)00259-9
75. Saito T, Oba T, Shimizu S, Asada A, Iijima KM, Ando K (2019) Cdk5 increases MARK4 activity and augments pathological tau accumulation and toxicity through tau phosphorylation at Ser262. Hum Mol Genet 28(18):3062–3071. https://doi.org/10.1093/hmg/ddz120
76. Wei FY, Nagashima K, Ohshima T, Saheki Y, Lu YF, Matsushita M et al (2005) Cdk5-dependent regulation of glucose-stimulated insulin secretion. Nat Med 11(10):1104–1108. https://doi.org/10.1038/nm1299
77. Wu H, Wu ZG, Shi WJ, Gao H, Wu HH, Bian F et al (2019) Effects of progesterone on glucose uptake in neurons of Alzheimer's disease animals and cell models. Life Sci 238:116979. https://doi.org/10.1016/j.lfs.2019.116979
78. Li X, Han H, Hou R, Wei L, Wang G, Li C et al (2013) Progesterone treatment before experimental hypoxia-ischemia enhances the expression of glucose transporter proteins GLUT1 and GLUT3 in neonatal rats. Neurosci Bull 29(3):287–294. https://doi.org/10.1007/s12264-013-1298-y
79. Guiochon-Mantel A, Lescop P, Christin-Maitre S, Loosfelt H, Perrot-Applanat M, Milgrom E (1991) Nucleocytoplasmic shuttling of the progesterone receptor. EMBO J 10(12):3851–3859
80. Hagan CR, Daniel AR, Dressing GE, Lange CA (2012) Role of phosphorylation in progesterone receptor signaling and specificity. Mol Cell Endocrinol 357(1–2):43–49. https://doi.org/10.1016/j.mce.2011.09.017
81. Boucher J, Kleinridders A, Kahn CR (2014) Insulin receptor signaling in normal and insulin-resistant states. Cold Spring Harb Perspect Biol. https://doi.org/10.1101/cshperspect.a009191